Research Article

Optimization Analysis of Controlled Blasting for Passing through Houses at Close Range in Super-Large Section Tunnels

Zhanping Song [iD],[1,2] **Jianchao Mao** [iD],[1,2] **Xiaoxu Tian** [iD],[1,2] **Yuwei Zhang** [iD],[1,2] **and Junbao Wang** [iD][1,2]

[1]*School of Civil Engineering, Xi'an University of Architecture and Technology, Xi'an, Shaanxi 710055, China*
[2]*Shaanxi Key Laboratory of Geotechnical and Underground Space Engineering, Xi'an University of Architecture and Technology, Xi'an 710055, China*

Correspondence should be addressed to Zhanping Song; songzhpyt@xauat.edu.cn and Yuwei Zhang; 1032659676@qq.com

According to the on-site vibration velocity monitoring and peak vibration velocity prediction, it is found that the maximum vibration velocity generated by the existing Dizong blasting scheme does not meet the requirements of the maximum allowable vibration velocity of houses. Therefore, the existing blasting scheme is optimized by reducing the maximum single-segment charge and a variety of damping measures such as multistage duplex wedge groove, adding damping hole, and millisecond blasting. In addition, the blasting data before and after optimization are analyzed and compared by wavelet (packet) technology. The results show that the optimized blasting main frequency domain is increased to 50~150 Hz and the maximum vibration intensity value is reduced by 79.8%. Based on the time-energy analysis, the maximum energy value is reduced by 67.75% compared with the original scheme, and the dominant energy of the original scheme is reduced by 97.81%, 71.49%, 82.44%, 95.93%, and 93.03%, respectively, after optimization. The maximum vibration velocity generated by the optimized blasting scheme construction is 1.12 cm/s, which is less than the maximum allowable vibration velocity of the building of 1.2 cm/s, which meets the maximum allowable vibration velocity requirements of the building. The optimized blasting scheme realizes the safe and rapid construction of the two steps of the Dizong tunnel, which can provide a reference for similar engineering construction in the future.

1. Introduction

With the rapid development of China's traffic construction, the construction problems of tunnels passing through the existing buildings (structures) at close range will appear in large numbers [1–4]. For tunnels constructed by drilling and blasting, the seismic waves generated by blasting will cause vibration of the buildings (structures) when it propagates to the ground and may cause cracking or even collapse of the buildings (structures) [5–8]. Therefore, studying the propagation law of tunnel blasting vibration in the formation, and optimizing the blasting scheme based on this, has important practical significance for controlling the blasting vibration effect and ensuring the safety of adjacent buildings (structures) [9–11].

In terms of the propagation law of blasting vibration, based on a large amount of monitoring data, Nateghi [12]

studied the impact of different rock formations, different detonators, and explosives on the surface movement caused by blasting vibration near the underground and surface concrete structures during the construction of the upper Gotvand dam. Lee et al. [13] proposed a precut discontinuity similar to the presplitting around the tunnel to study the attenuation of wave propagation caused by the blasting of the tunnel. The results showed that the attenuation reduction coefficient with an ideal cutoff discontinuity was 50%. Wang et al. [14] used the LS-DYNA program to study the propagation characteristics represented by the time-space change of surface acceleration. The results show that the maximum main stress decreases with the increase in the distance from the source. Chen et al. [15] used the separation variable method to solve the displacement potential function of blasting vibration wave propagation and obtained the

variation law of particle movement and stress with axial distance, radial distance, and time in the surrounding rock.

In the aspect of vibration reduction of tunnel blasting, Ozacar [16] determined the most suitable time delay in the blast hole group to destructively interfere with the surface wave at the target position and reduce the ground vibration caused by the explosion at the target position. Kim and Song [17] used abrasive water jet cutting technology to reduce the ground vibration caused by tunnel excavation blasting. Through experimental and numerical studies, this method can effectively reduce the ground vibration caused by blasting. Liang et al. [18] studied the influence of blasting vibration of Xinjiang new railway tunnel on the existing tunnels. Based on the results of on-site monitoring and numerical simulation, the original blasting design and corresponding parameters were adjusted to reduce the surface vibration caused by blasting. Li et al. [19] adopted a series of technical measures to reduce vibration in the blasting excavation of Nanjing Hongshan Highway Tunnel, which reduced the impact of blasting vibration on subway tunnels and catenaries, and ensured the safe operation of the subway. Li and Li [20] used the finite element method to compare and analyze the CD method, the step method, and the reserved core soil in the blasting excavation method and determined the damping excavation method for shallow buried tunnels crossing dense residential areas. Xie et al. [21] used LS-DYNA software to simulate six different types of blasting excavation methods. By analyzing them, a reasonable blasting excavation method was proposed to reduce blasting vibration.

All the above scholars have made an in-depth and beneficial exploration on the propagation law and vibration reduction technology of tunnel blasting. However, the current study mostly focuses on the blasting vibration reduction technology of urban metro tunnels passing through the existing tunnel in a short distance [22–25]. There are few studies on controlled blasting technology of super-large section mountain tunnel excavated by the two-step method under close-distance crossing dense buildings. Therefore, based on the propagation law of the tunnel blasting vibration in the stratum, it is very necessary to study the blasting vibration reduction technology of super-large section tunnel excavated by the two-step method under existing buildings for the realization of efficient, rapid, and safe construction of tunnels.

This paper takes the underground tunnel of the Dizong tunnel as the engineering background, tests the vibration velocity under different blasting distances, and analyzes the propagation law of blasting vibration velocity in the stratum. According to the analysis, the maximum vibration velocity generated by the existing blasting scheme does not meet the requirements of the maximum allowable vibration of the house, and an optimization scheme which combines the control of single-segment maximum charge, multistage duplex wedge groove, adding damping hole, and millisecond blasting was put forward in this paper. The wavelet (packet) analysis technology is used to compare and analyze the power spectrum characteristics, energy distribution characteristics, and time-energy variation rules of blasting signals before and after optimization. The optimized blasting scheme realizes the safe and rapid construction of the two steps of the Dizong tunnel, which can provide a reference for similar engineering construction in the future.

2. Engineering Overview

The newly constructed An-Liu high-speed railway is an intercity high-speed railway connecting cities of Anshun and Liupanshui, Guizhou, China. The Dizong tunnel is located in Liuzhi Special Zone and is an important node project of the ALTJ-2 section of the An-Liu High-speed Railway Station, as shown in Figure 1. The two-lane tunnel is of 3045 m long and has a 3.6 m wide median strip. According to the standards of the International Tunneling Association, the tunnel belongs to the super-large section tunnel ($158 \, m^2 > 100 \, m^2$).

The tunnel passes through the mountainous area of Chashan Village. There are 12 households near the DK41 + 945~DK42 + 100 (155 m) section. The total building area is 2311.25 m^2. The relationship between the specific buildings and the tunnel plane is shown in Figure 2. The buildings on the left side of the tunnel are relatively dense, mainly 1~3 stories, mostly brick-concrete buildings, lime-fly ash block stone structures, and bottom lime-fly ash block stones; the above buildings are strip foundations, the structure of the houses is not strong, the seismic resistance and mechanical performance are very poor, and some of them are already dangerous buildings themselves. Therefore, the tunnel blasting construction poses a certain threat to the safe use of the building in this section. Once the vibration speed is too high or the main frequency of blasting vibration is close to the natural frequency of the building, it may lead to the destruction of the building and cause accidents [26–28].

3. Blasting Scheme and Monitoring

3.1. Blasting Scheme Design. The buried depth of the tunnel in the DK41 + 945~DK42 + 000 section is 49~57 m, and the horizontal distance from the building is 45~80 m. The tunnel is a control project. Considering the above factors and construction period requirements, the blasting excavation construction adopts a two-step method. The upper step is 2.0 m per cycle, and the lower step is 3.0 m per cycle.

According to the site situation, the YT-28 rock drill with a one-shaped alloy drill bit of a 40 mm diameter is used. The explosive uses RJ-2 waterproof emulsion explosive with a diameter of 32 mm. The ordinary millisecond detonating industrial No. 8 detonator with 1–15 segments is used in separate sections. The layout of the blast hole on the upper step: the around blast hole spacing is 50 cm, the inner ring blast hole spacing is 120 cm, the vertical spacing of the cut blast hole is 20 cm, and the floor blast hole is 100 cm. The smooth blasting technique is used. The around blast holes are taken by noncoupling charge, and the interval component is loaded. The blast hole arrangement is shown in Figure 3, and the blasting design parameters are shown in Tables 1 and 2.
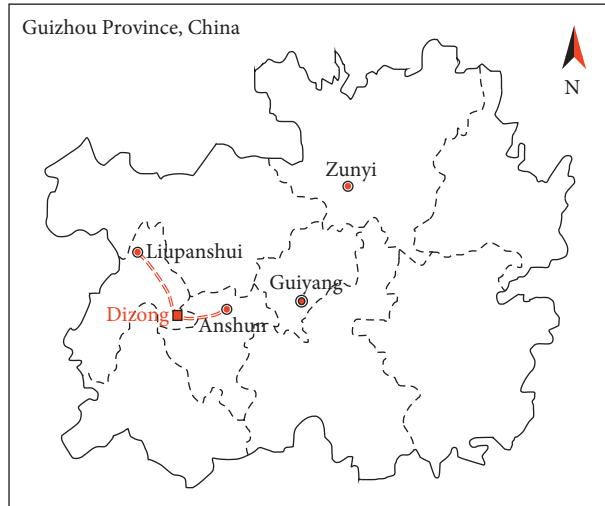
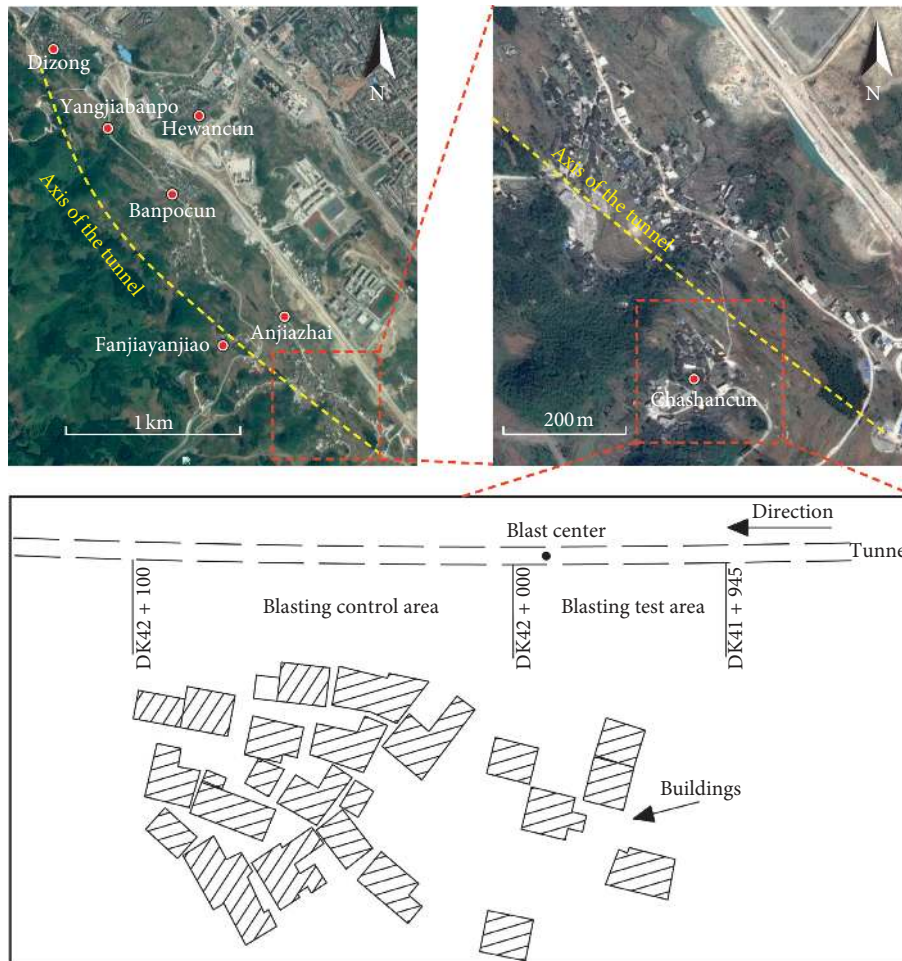FIGURE 1: Schematic diagram of the location of the Dizong tunnel.

FIGURE 2: Diagram of the relationship between buildings and tunnel.

3.2. Vibration Monitoring. When the tunnel is excavated to DK41 + 945~DK42 + 100 section, the enhanced TC-4850 blasting vibration measuring instrument with high accuracy and strong applicability is used for monitoring. The instruments are installed at 23 m, 26 m, 29 m, 32 m, 36 m, 41 m, 47 m, and 53 m above the central line of the tunnel in the blasting test area and at the corner of the houses closest to the blast-heart in the blasting control area, as shown in
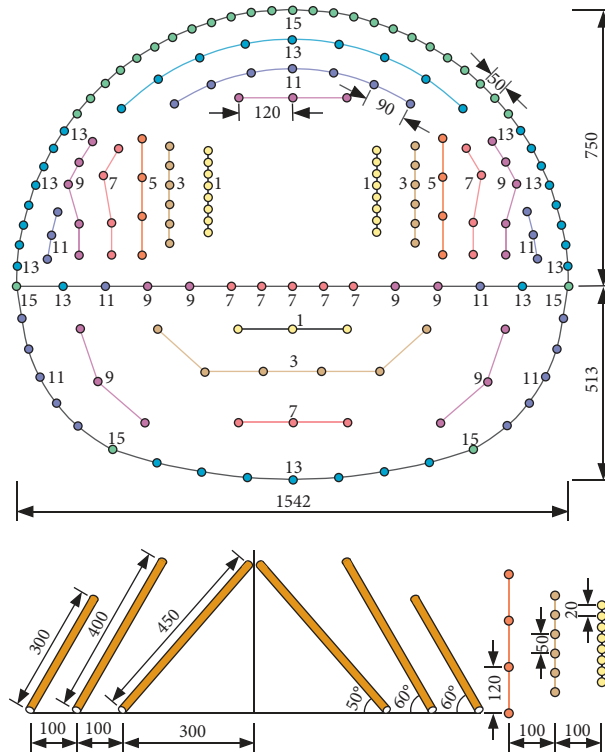
FIGURE 3: Blast hole layout (unit: cm). Note: the number in the figure is the detonator segment.

TABLE 1: Parameters of the upper step blasting.

Detonator segment	Hole depth (m)	Hole number	Blast hole name	Explosive charge per hole (kg)	Single-stage charge (kg)
1	4.5	16	Cutting hole	1.5	24
3	4	12	Driving hole	1.2	14.4
5	3	8	Driving hole	0.9	7.2
7	3	8	Driving hole	0.9	11.7
7	3	5	Floor hole	0.9	
9	3	7	Driving hole	0.9	
9	3	6	Inner ring hole	0.9	15.3
9	3	4	Floor hole	0.9	
11	3	6	Inner ring hole	0.9	
11	3	2	Floor hole	0.9	13.5
11	3	7	Driving hole	0.9	
13	2	8	Around hole (odd)	0.3	
13	2	8	Around hole (even)	0.6	17.1
13	3	9	Inner ring hole	0.9	
13	3	2	Floor hole	0.9	
15	3	2	Floor hole	1.2	
15	3	12	Around hole (odd)	0.3	13.8
15	3	13	Around hole (even)	0.6	
Total	—	135	—	—	116.4

Figure 4. Each vibrometer has three channels, of which the horizontal direction is X and Y and the vertical direction is Z. It can collect the velocity, frequency, and duration of three different directions at the same time.

In the DK41 + 945~DK42 + 000 section, the vertical vibration waveform of the upper step of the measuring point T-1 is shown in Figure 5, the relationship between the vibration velocity of the upper and lower steps and the blast center distance is shown in Figures 6 and 7, respectively, and

the distribution of the main frequency and the blast center distance of the upper and lower steps is shown in Figure 8.

Analysis of Figure 5 shows that the millisecond blasting technology can realize the peak staggering and interference of the blasting vibration wave. The maximum vibration velocity is mainly caused by the explosion of the first segment explosive (the cut blasting). Compared with other segment blast holes, the single-segment charge of the cutting holes is the largest, and there is only one vacant surface when

TABLE 2: Parameters of the lower step blasting.

Detonator segment	Hole depth (m)	Hole number	Blast hole name	Explosive charge per hole (kg)	Single-stage charge (kg)
1	5	3	Driving hole	1.2	3.6
3	5	6	Driving hole	1.2	7.2
7	5	3	Driving hole	1.5	4.5
9	5	6	Auxiliary hole	1.5	9
11	4.5	10	Around hole	0.9	9
13	4.5	7	Around hole	2.1	14.7
15	4.5	2	Around hole	2.1	4.2
Total	—	37	—	—	52.2

Note: the around hole of the upper section is filled with spacer charge (1 for odd holes and 2 for even holes).
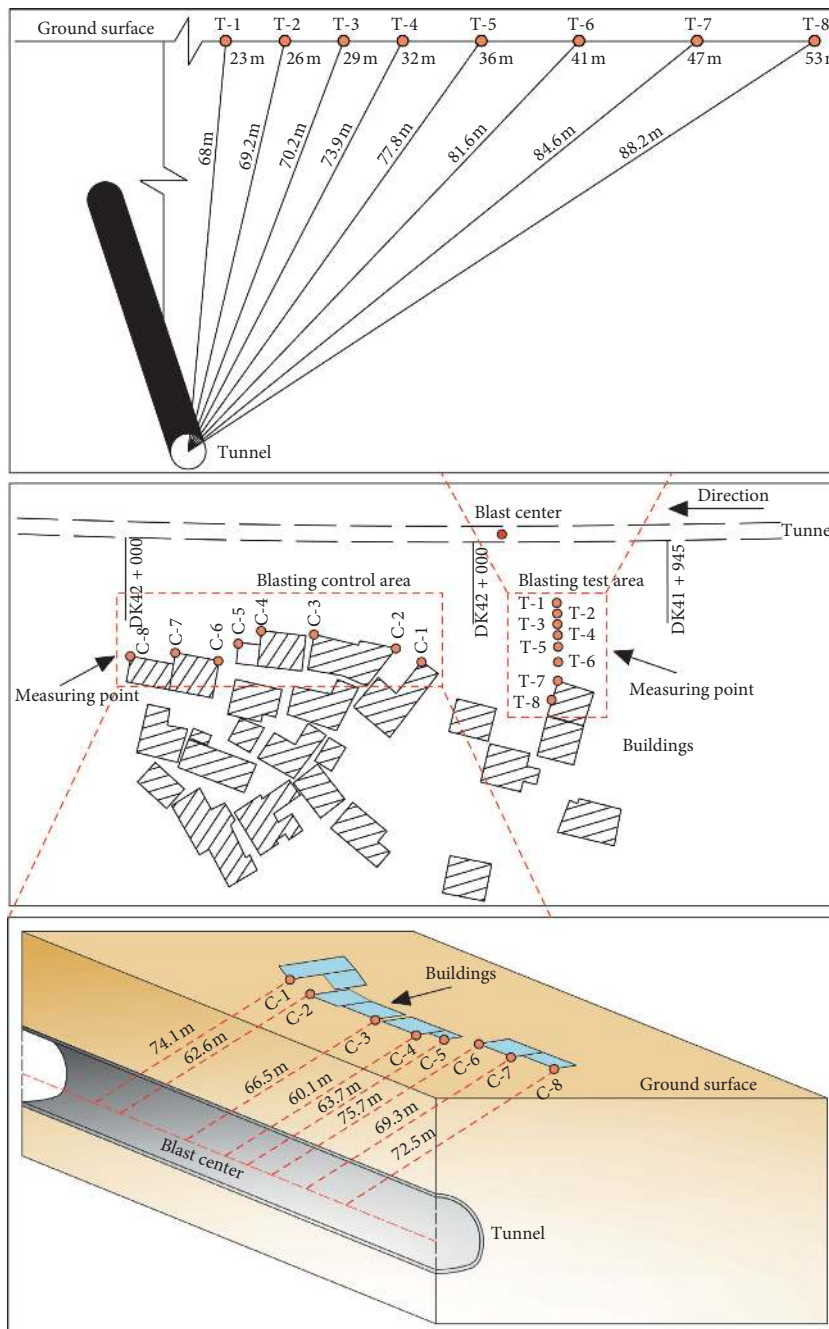

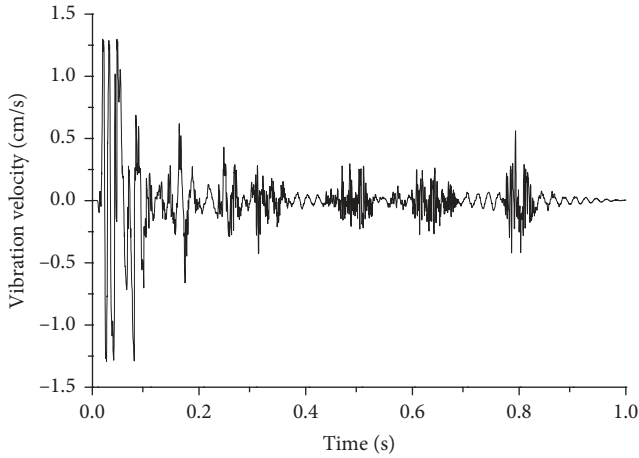FIGURE 4: Layout of the vibration monitoring points.

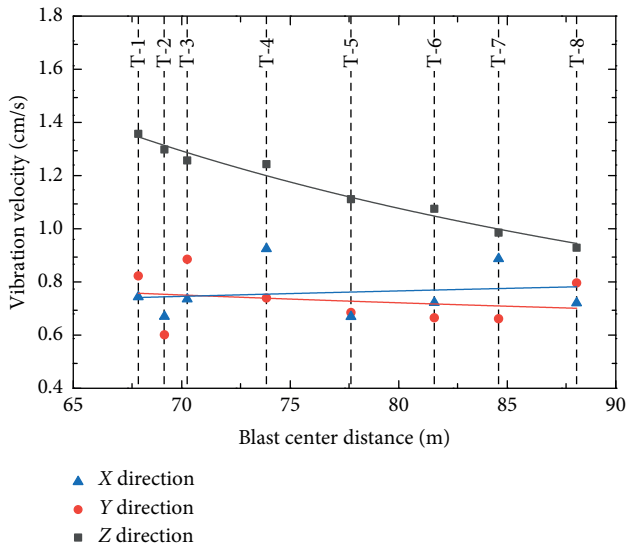Figure 5: Vertical vibration waveform of the upper step at T-1.

Figure 6: Relationship between the vibration velocity and the blast center distance of the upper step.
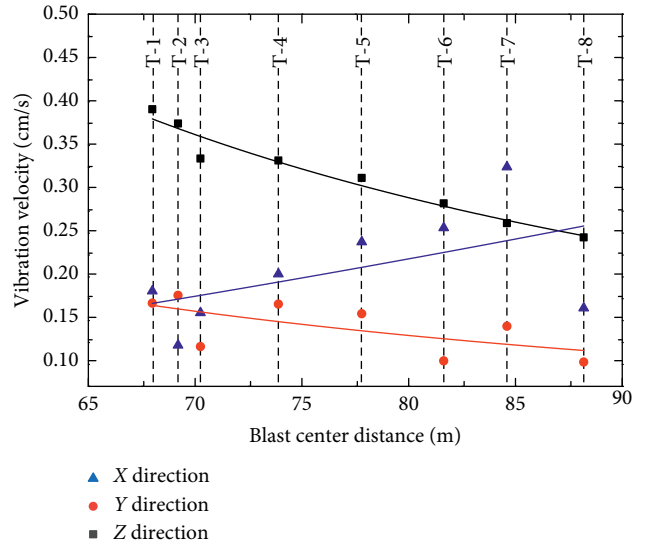

Figure 7: Relationship between the vibration velocity and the blast center distance of the lower step.

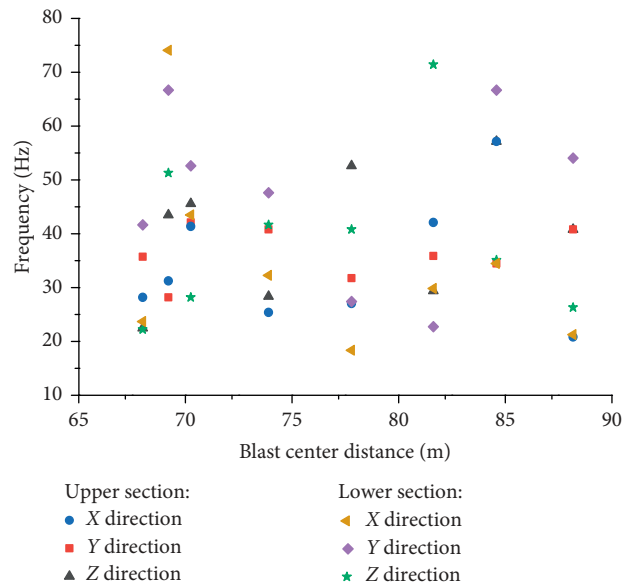Figure 8: Distribution of the main frequency with the blast center distance of the upper and lower steps.

blasting. Therefore, it is very important to control the maximum single-segment charge and create the vacant surface as much as possible to reduce the blasting vibration.

Analysis of Figures 6 and 7 shows that the vertical value of the three-channel vibration velocity is greater than the horizontal direction, and the vertical vibration velocity is more affected by the blast center distance. Therefore, the vertical vibration velocity can be the main criterion for the vibration velocity control, and the vertical vibration velocity should be noted during the monitoring process. The vertical vibration velocity of the upper step is mostly between 0.8 and 1.4 cm/s, and the vertical vibration velocity of the lower step is mostly between 0.1 and 0.4 cm/s, indicating that the upper step blasting is the main factor affecting the safety of the building. The main reason for the large vibration caused by the upper step blasting is that the single-segment charge of the cutting holes in the upper step blasting is larger, and the excavation section is larger, and the rock clip is stronger. Compared with the upper step, the blasting of the upper step

during the blasting of the lower step has already produced a vacant surface for it, and thus the vibration caused by the blasting of the lower step is small.

Analysis of Figure 8 shows that the main frequency of the blasting vibration wave is between 20 and 80 Hz. The general building structure is less than 10 Hz [29], so the blast will not cause resonance in the house.

3.3. Regression Analysis of Vibration Parameters Based on Blasting Vibration Test. At present, Sadovsky's empirical attenuation formula is the most widely used in engineering and can better reflect the attenuation law of blasting vibration [30, 31]. The formula is as follows:

$$V = K\left(\frac{\sqrt[3]{Q}}{R}\right)^{\alpha}, \tag{1}$$

where V is the vibration velocity (cm/s), Q is the charge (kg), R is the blast center distance (m), and K and α are the coefficients related to site conditions.

In order to continuously optimize the blasting design scheme and scientifically guide the blasting construction of the tunnel passing through buildings, according to the field measured data, the least squares method is adopted for the regression analysis of formula (1) [32]. $K = 198.1$ and $\alpha = 1.581$ can be obtained by calculation, and the regression curve is shown in Figure 9.

Therefore, Sardonsky's empirical formula is

$$V = 198.1\left(\frac{\sqrt[3]{Q}}{R}\right)^{1.581}. \tag{2}$$

The blasting vibration safety allowable charge formula can be obtained by changing Sardonsky's empirical formula:

$$Q = R^3\left(\frac{V}{198.1}\right)^{3/1.581}. \tag{3}$$

Each symbol in the formula has the same meaning as above.

3.4. Problems with the Blasting Scheme. By monitoring the blasting test area, it can be found that the vibration velocity is between 1.2 and 1.4 cm/s while the blasting distance is between 65 and 70 m. According to the "GB 6722-2014 Safety Regulations for Blasting" and considering that the blasting seismic wave will produce amplification effect on the second and third floors of the building [33, 34], it is determined that the maximum allowable vibration velocity is 1.2 cm/s. So the vibration velocity of the test area has not met the specifications. On the contrary, the peak velocity prediction of the blasting control area: The buried depth of the tunnel in the DK42 + 000~DK42 + 100 section is 39~50 m, the horizontal distance from the building is 25~35 m, the blast center distance is smaller, and the minimum blast center distance is 60 m. Calculate the maximum vibration velocity according to formula (2), in which the maximum single-segment charge is 24 kg, the blasting-center distance is 60 m, and the maximum vibration velocity is 1.63 cm/s. It can be found that the predicted vibration velocity of the blasting control area has also exceeded the allowable value of the specification. Combined with on-site monitoring and peak vibration velocity prediction, it is clear that the original blasting scheme has not met the requirements of the specification. Therefore, in order to ensure the safe use of the building, the blasting design needs to be optimized.

4. Optimization of Controlled Blasting Scheme for Close Crossing Buildings

4.1. The Determination of the Single-Segment Charge. From the vibration monitoring analysis of the blasting test area, it can be known that the maximum vibration velocity is
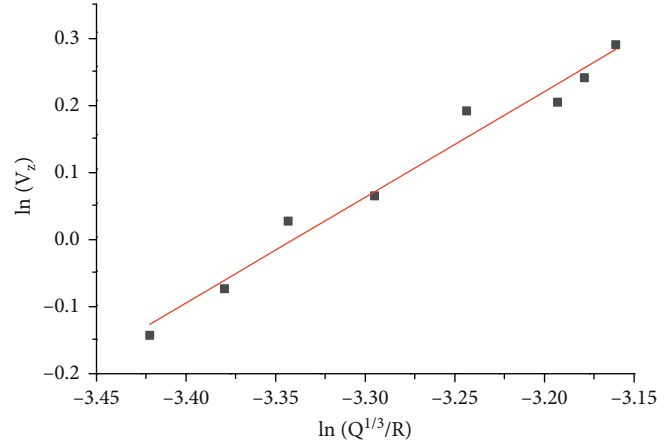

FIGURE 9: Least squares regression curve of blasting data.

caused by the cutting holes, and it is necessary to control the maximum single-segment charge of the cut blasting. However, this project should not reduce the footage, so as not to affect the effect of the blasting, the maximum vibration velocity of the blasting is 1.5 m/s. The maximum single-segment charge is calculated by using the formula (3), wherein the minimum blast center distance is 60 m, and the maximum single-segment charge can be calculated to be 20.4 kg.

4.2. Earthquake Reduction Technology and Design Scheme

4.2.1. Multistage Double Wedge Groove. Although the effect of single-stage large wedge cut blasting is better, the vibration intensity produced by single-stage large wedge cut blasting is very strong because of the large number of explosives and the strong effect of rock clamping. At present, the main cutting methods that can effectively reduce blasting vibration in tunnel blasting are the straight hole cutting with large diameter empty holes and the multistage double wedge groove. However, the straight hole cutting with large diameter empty holes requires a large diameter drill, which has strict requirements on drilling accuracy. Due to the technical level of mechanical equipment and drilling personnel, mountain tunnel is rarely used. The multistage double wedge groove can reduce the charge of all levels of cutting, and the upper level cut blasting can produce the free surface for the lower level cut blasting, which greatly reduces the effect of rock clamping. In addition, the multistage double wedge groove has strong applicability and can be adjusted timely according to the site construction conditions, which has low requirements for drilling accuracy, the good effect of rock throwing, and low consumption of explosives. Therefore, the multistage double wedge groove is used to optimize the single-stage large wedge groove, as shown in Figure 10.

4.2.2. Adding Empty Holes. Adding empty holes in the cut blasting can provide the free surface for blasting, reduce the effect of rock clamping, increase the compensation space for rock fracture and expansion, and change the local resistance
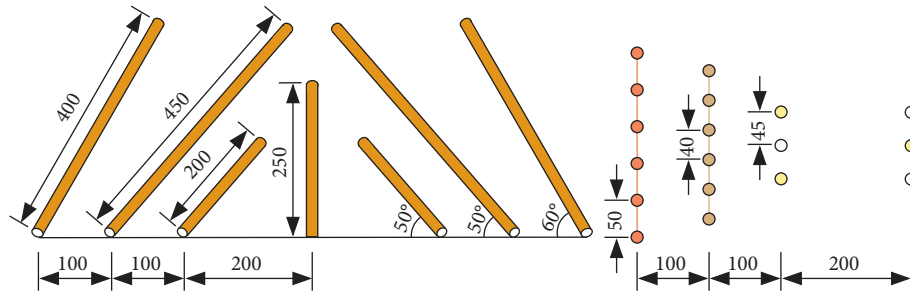
FIGURE 10: Layout of multistage double wedge groove (unit: cm).

line, which is beneficial to the effect of grooving. Therefore, empty holes are added in the design of the cut blasting [35].

4.2.3. Set the Damping Holes. The propagation characteristics of blasting seismic waves mainly depend on the wave impedance characteristics of the medium. When the tunneling excavation profile is provided with damping holes and the blasting vibration wave reaches the damping holes, the vibration wave will generate reflection and transmission due to the difference in the wave impedance characteristics. The tensile wave will return to the blast zone, a portion of the compression wave will be transmitted, and the transmitted wave intensity will be weakened, thereby reducing the vibration behind the isolation band [36].

4.2.4. Blasting Design Scheme. After determining the above optimization method, the blasting optimization design of the upper step is carried out. The layout of the blasting blast hole after optimization design of the upper step is shown in Figure 11, and the parameters of the upper step after blasting optimization are shown in Table 3.

5. Results and Discussion

5.1. Field Test of Controlled Blasting Vibration under the Houses. In the DK42 + 000~DK42 + 100 section, the vertical vibration waveform of the upper step of the measuring point C-3 is shown in Figure 12, the relationship between the vibration velocity of the upper and lower steps and the blast center distance is shown in Figures 13 and 14, respectively, and the distribution of the main frequency and the blast center distance of the upper and lower steps is shown in Figure 15.

Analysis of Figures 5 and 12 shows that the maximum vibration velocity of blasting is still mainly caused by the cut blasting, but due to multistage double wedge-shaped groove blasting, the vibration caused by blasting has several peaks. It can be seen that the maximum vibration velocity of blasting occurs in the two-stage cut blasting (the third-segment blasting). The maximum vibration velocity generated is greatly reduced before the optimization of the cut blasting, and the vibration velocity generated by each blasting is significantly reduced, indicating that the damping hole technology reduces the blasting vibration during the blasting vibration propagation process.

It can be seen from Figures 13–15 that the maximum vibration velocity generated by the blasting design is 1.12 cm/s, which is lower than the vibration velocity control standard value of 1.2 cm/s, and the horizontal vibration velocity is smaller than the vertical vibration velocity. The vertical vibration velocity of the upper step is mostly between 0.75 and 1.12 cm/s, while the vertical vibration velocity of the lower step is mostly between 0.1 and 0.45 cm/s. Compared with the original scheme, there is no significant change in the lower step. The damping holes around the upper step do not reduce the vibration generated by the lower step blasting. The main frequency of blasting vibration is between 20 and 95 Hz. Therefore, the above optimized damping measures can effectively control the blasting vibration, avoiding the resonance of the house and achieving the goal of 2 m per cycle.

5.2. Power Spectrum Analysis. The FFT and power spectrum calculation program of blasting vibration signal are programmed by using MATLAB software. The vertical signals before and after optimization are calculated. The power spectral density maps are, respectively, shown in Figures 16 and 17, respectively.

It can be seen from Figures 16 and 17 that the blasting vibration signal is widely distributed in the frequency domain, and there are multiple dominant frequencies in the main frequency domain. Before optimization, the main frequency domain is basically between 20~110 Hz, and the dominant frequencies are 27, 35, 51, 59, 82, and 101 Hz. After the blasting optimization scheme, the main frequency domain is increased between 50 and 225 Hz and mainly concentrated between 50 and 150 Hz, mainly concentrating in the high-frequency region, and the dominant frequencies are 54, 76, 117, 150, and 201 Hz. Therefore, it can be seen that the frequency generated by the blasting control technology is much higher than the natural vibration frequency of the house and does not cause resonance.

By comparing the variation law of PSD, it can be known that the vibration intensity before optimization is mainly concentrated in the range of 0~110 Hz, the intensity value is large, and the maximum intensity value is 0.001616. After the blasting optimization scheme, the distribution of vibration intensity in the frequency domain is further developed to high frequency, and the intensity value is greatly reduced. The maximum intensity value is 0.000326, which is 79.80% lower than that before optimization. It can be seen that the
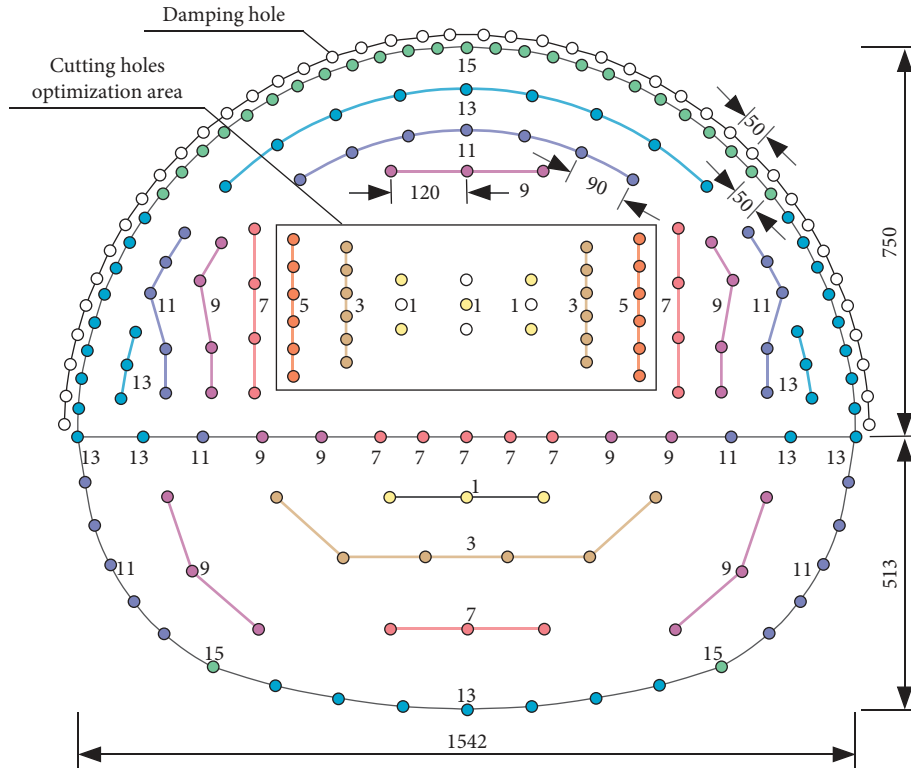
FIGURE 11: Layout of the blast hole of the upper step after optimization design. Note: the number in the figure is the detonator segment.

TABLE 3: Parameters of the upper step after optimization.

Detonator segment	Hole depth (m)	Hole number	Blast hole name	Explosive charge per hole (kg)	Single-stage charge (kg)
1	2.5	1	Cutting hole	1.2	4.8
1	2	4	Cutting hole	0.9	
3	4.5	12	Cutting hole	1.5	18
5	4	12	Cutting hole	1.2	14.4
7	3	8	Driving hole	0.9	11.7
7	3	5	Floor hole	0.9	
9	3	11	Driving hole	0.9	13.5
9	3	4	Floor hole	0.9	
11	3	11	Driving hole	0.9	
11	3	6	Inner ring hole	0.9	17.1
11	3	2	Floor hole	0.9	
13	3	15	Inner ring hole	0.9	
13	3	2	Floor hole	0.9	17.7
13	3	2	Floor hole	1.2	
15	3	21	Around hole (odd)	0.3	18.3
15	3	20	Around hole (even)	0.6	
—	—	42	Damping hole	—	—
—	—	4	Empty hole	—	—
Total	—	182	—	—	115.5

Note: the around hole of the upper section is filled with spacer charge (1 for odd holes and 2 for even holes).

optimization scheme can effectively reduce the vibration intensity.

5.3. Time-Energy Analysis. When using MATLAB software to write the program, the db7 wavelet base is used for wavelet analysis. The upper limit of the integral is 15 and the lower limit of the integral is 1. The distribution of energy in time from 0 to 150 Hz is obtained. The signal time-energy distribution before and after blasting optimization is shown in Figures 18 and 19, respectively.

It can be seen from Figures 18 and 19 that because the original blasting scheme has the largest single-segment charge in the cutting holes, and there are fewer free surfaces during blasting, the blasting energy is mainly concentrated in the first segment cut blasting (0~50 ms). After using the
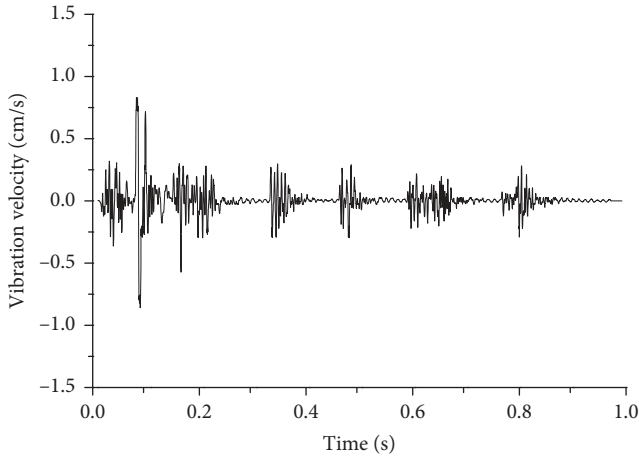
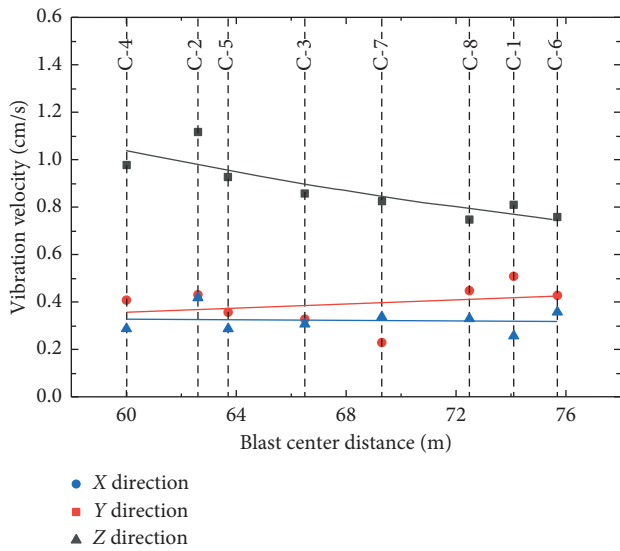FIGURE 12: Vertical vibration waveform of the upper step at C-3.

FIGURE 14: Relationship between the vibration velocity and the blast center distance of the lower step.

FIGURE 13: Relationship between the vibration velocity and the blast center distance of the upper step.
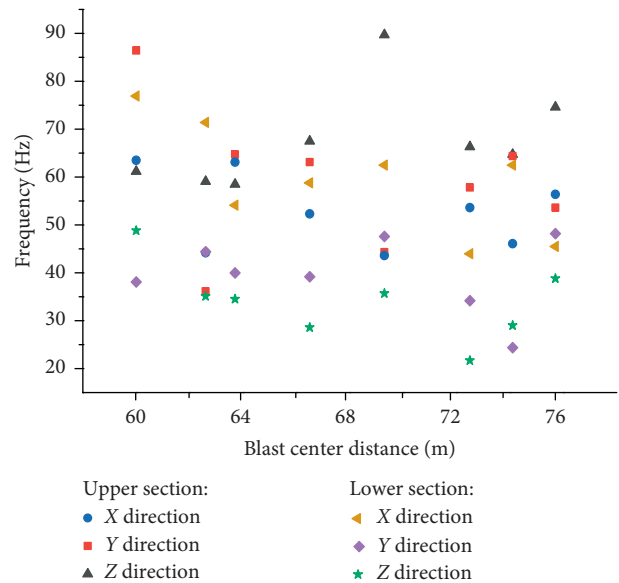
FIGURE 15: Distribution of the main frequency with the blast center distance of the upper and lower steps.

blasting control technology, although the blasting energy mainly comes from the cut blasting (0~200 ms), the maximum energy value of the blasting vibration signal has been reduced by 67.75%, and the maximum energy peak appears in the second segment cut blasting. In addition, the blasting energy values of subsequent segments are small. Therefore, it is important to control the maximum single-segment explosive volume and create a free-facing surface as much as possible to reduce the blasting vibration.

During the change of blasting energy with time, the energy value has multiple peaks. Each time a peak appears, the energy at the corresponding moment has a sudden change. At this moment, the explosive is detonated. Compared with the burst delay time (Table 4), it can be found that the time corresponding to the energy peak is basically consistent with the delay time of the blasting detonator, which indicates that the optimized blasting scheme can
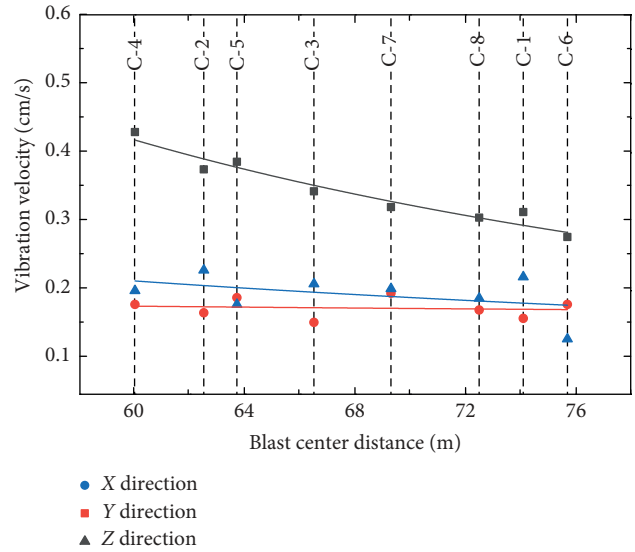
effectively realize the delayed release of blasting energy and the staggered peak of blasting vibration.

5.4. Vibration Velocity and Energy Analysis Based on Wavelet Packet. Wavelet packet analysis can decompose the high and low frequencies of the signal together, with high resolution, and can realize the refined analysis of the blasting vibration signal. To this end, the wavelet packet analysis program is written by using MATLAB software, and db8 wavelet basis with tight support, smoothness, and symmetry was used to analyze the blasting vibration signal. Since the sampling rate is 2000 Hz, the Nyquist is 1000 Hz according
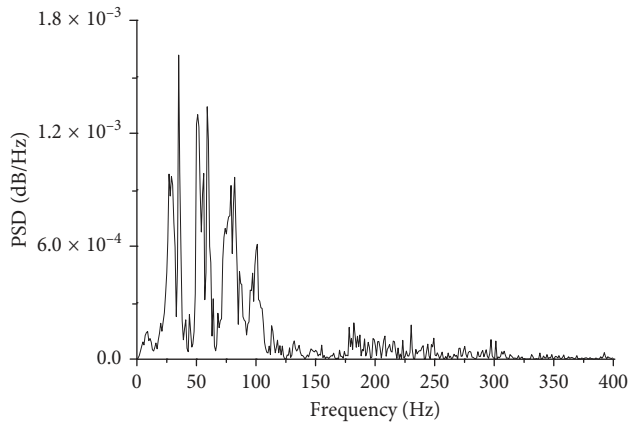
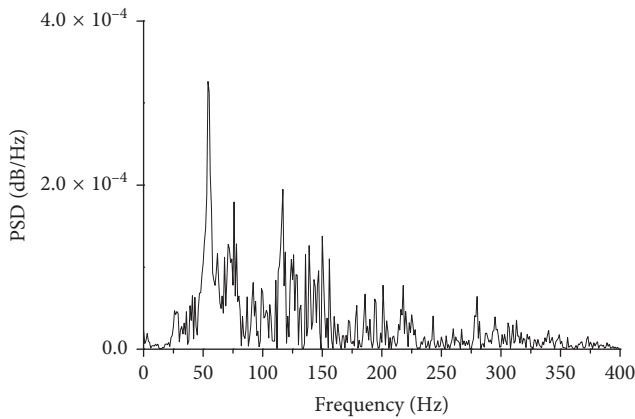FIGURE 16: Vertical power spectral density before optimization.

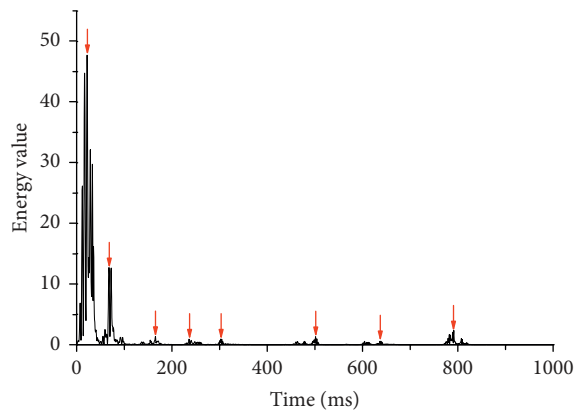FIGURE 17: Vertical power spectral density after optimization.

FIGURE 18: The time-energy distribution of the blasting before optimization.

to the sampling law. The number of decomposition layers is 6 layers, which are decomposed into 64 frequency bands, and each frequency band is 15.6 Hz. Taking the optimized vertical signal as an example, the wavelet packet decomposition reconstruction can obtain the signals of each frequency band, and 1~16 (0~249.6 Hz) band reconstruction signal is shown in Figure 20.
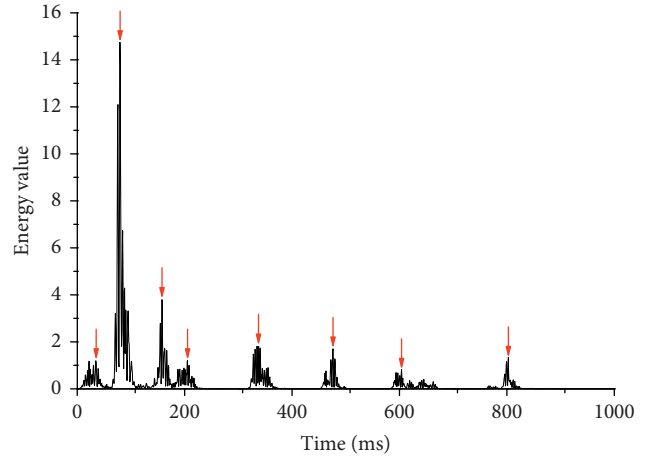

FIGURE 19: The time-energy distribution of the blasting after optimization.

5.4.1. Analysis of Vibration Velocity with Frequency Band. Because the blasting vibration safety criterion is not only related to the vibration speed, but also closely related to the frequency, and the safety criterion combined with the vibration frequency has become the main body in the current vibration safety evaluation system. Therefore, after the wavelet packet decomposition and reconstruction described above, by filtering out the maximum value of the vibration velocity of each frequency band, the distribution of the vertical maximum vibration velocity with the frequency band before and after optimization can be obtained, as shown in Figure 21.

It can be seen from Figure 21 that the maximum vibration velocity of the blasting signal before optimization corresponds to the low-frequency region, and multiple peaks appear in the distribution of the vibration velocity with the frequency band, but the frequency domain corresponding to the peak is not concentrated and dispersed. After optimization, except for the 10 bands, the maximum vibration velocity of other bands is reduced, and the frequency is developed in the high-frequency region, the number of peaks is significantly reduced, and the vibration velocity is relatively flat with the frequency band. Therefore, in the safety evaluation system based on vibration velocity and frequency, by optimizing the damping measures, the maximum vibration speed corresponding to the blasting frequency can fall within the allowable range, ensuring the safety of the building.

5.4.2. Analysis of Blasting Vibration Energy with Frequency Band. The above spectrum analysis shows that the main frequency domain of the optimized blasting vibration is 50~225 Hz. To study the energy distribution law of the blasting signal in the main frequency domain, the first 20 frequency bands (0~280 Hz) are selected for energy calculation and optimized before and after optimization. The distribution of energy percentage and energy value is shown in Figures 22 and 23.
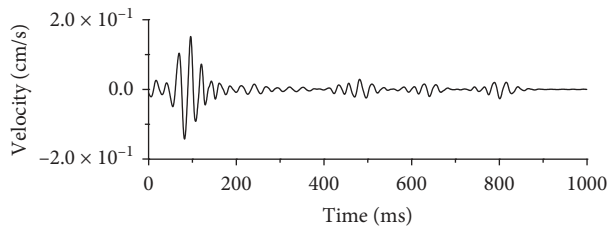
TABLE 4: Delay time of detonators.

Segment	1	3	5	7	9	11	13	15
Delay time (ms)	≤13	50	110	200	310	460	650	880
Error range (ms)	—	±10	±15	±20	±30	±40	±50	±60
Relative delay range (ms)	≤13	29–60	82–125	167–220	267–340	437–500	587–700	807–940
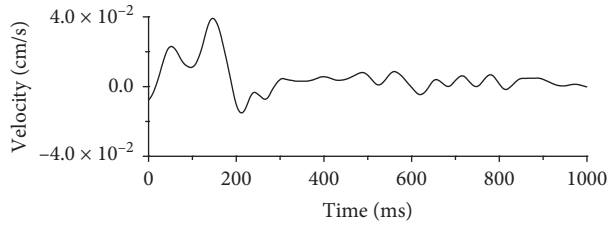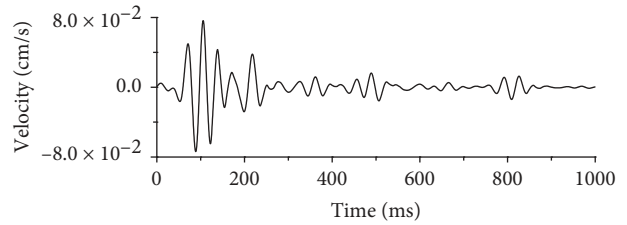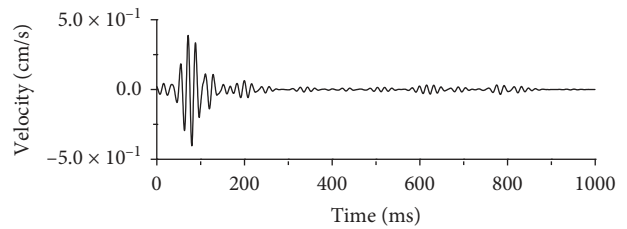
(a)

(b)

(c)

(d)

(e)

(f)

(g)
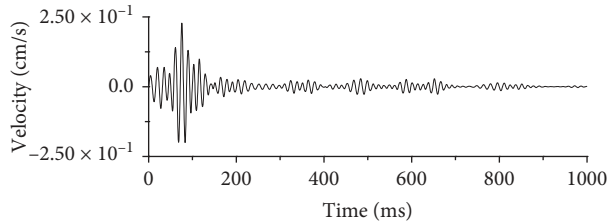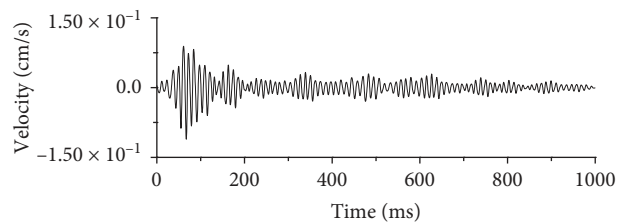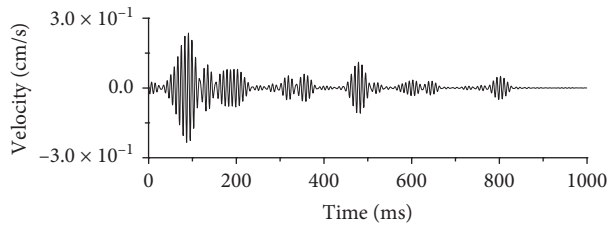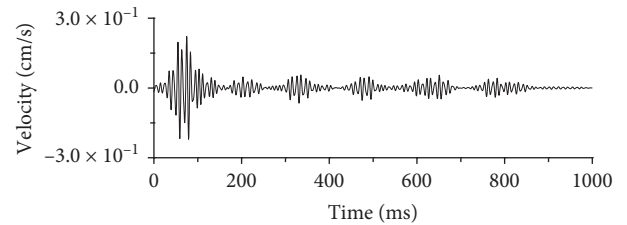
(h)

FIGURE 20: Continued.

Figure 20: Optimized vertical wavelet packet decomposition: 1–16 band reconstruction signal.

It can be seen from Figure 22 that the energy distribution is wider with the frequency domain, and a larger proportion appears in multiple frequency domains, indicating that the dominant energy of the blasting vibration is distributed in multiple frequency bands.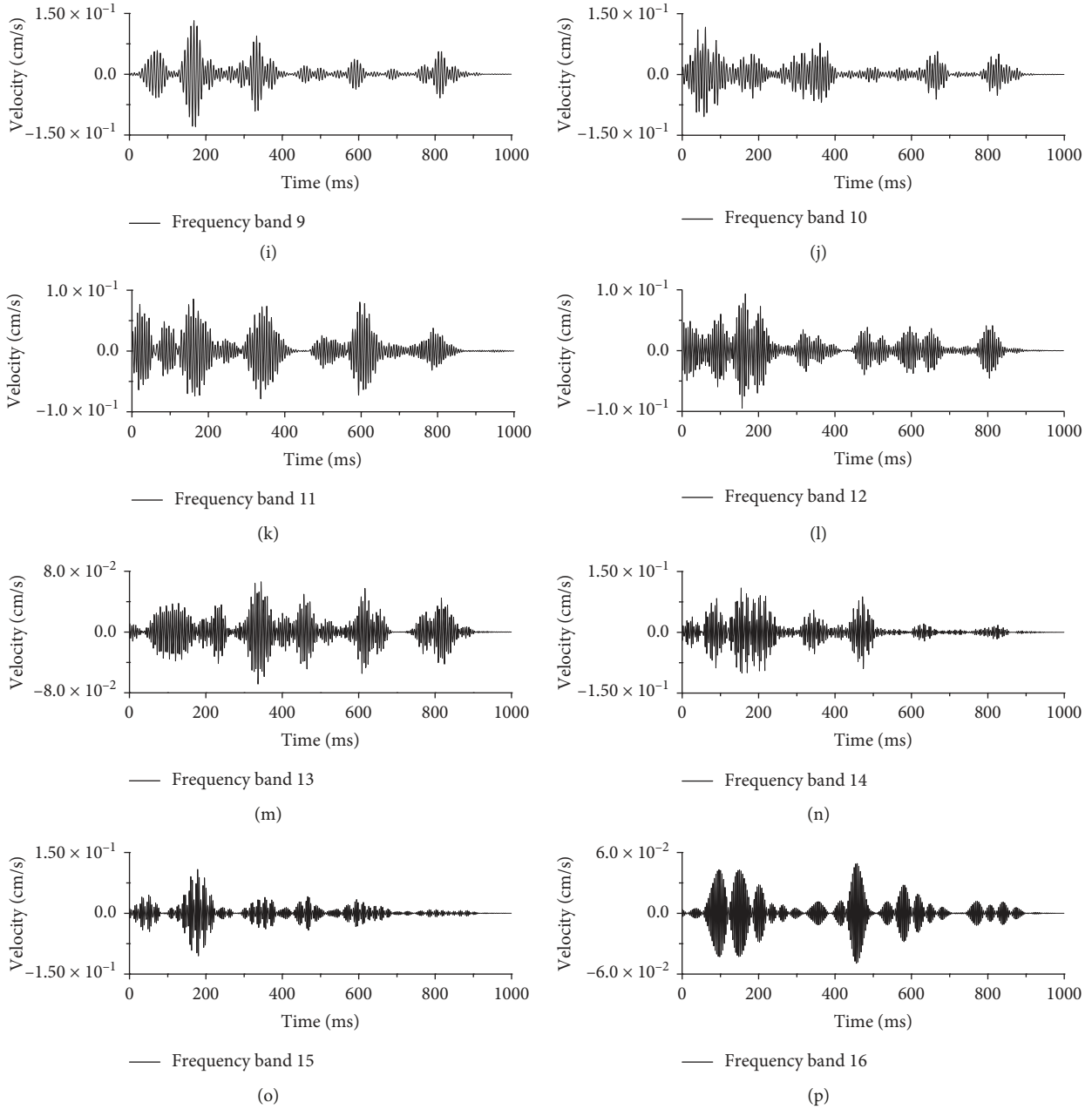 The energy of the original program blasting vibration signal is mainly distributed in the 2~8 frequency band (15.6~124.8 Hz), and the energy percentage is about 78.82%. The optimized energy is mainly distributed in the 3~14 frequency band (31.2~218.4 Hz), the energy percentage is about 79.71%; it also occupies a large part of the energy in the 18~20 frequency band, and the energy percentage is about 6.63%. It shows that the blasting vibration energy develops from low frequency to high frequency by controlled blasting technology.

It can be seen from Figure 23 that the energy concentration in the 2, 4, 5, 6, and 8 frequency bands occurs before optimization, and the energy values are 20.63, 35.43, 21.47, 17.22, and 28.56. After using the blasting control technology, the energy values of the corresponding frequency bands are 0.44, 10.10, 3.77, 0.70, and 1.99, and the percentage reductions are 97.81%, 71.49%, 82.44%, 95.93%, and 93.03%. It shows that the optimization scheme can greatly reduce the energy amplitude and reduce the energy concentration phenomenon.
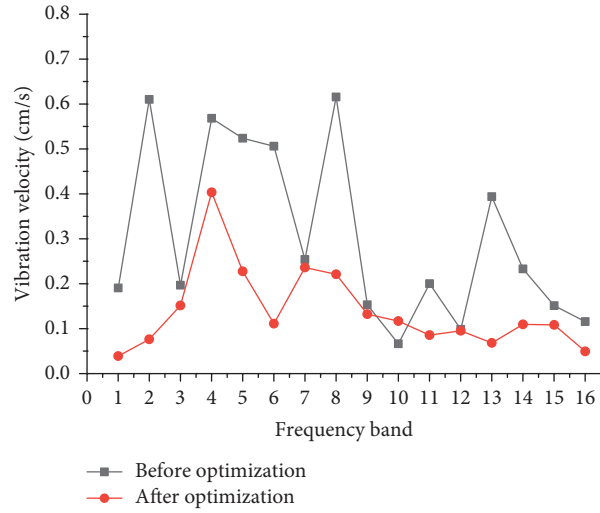
FIGURE 21: Vertical vibration velocity with frequency band distribution.
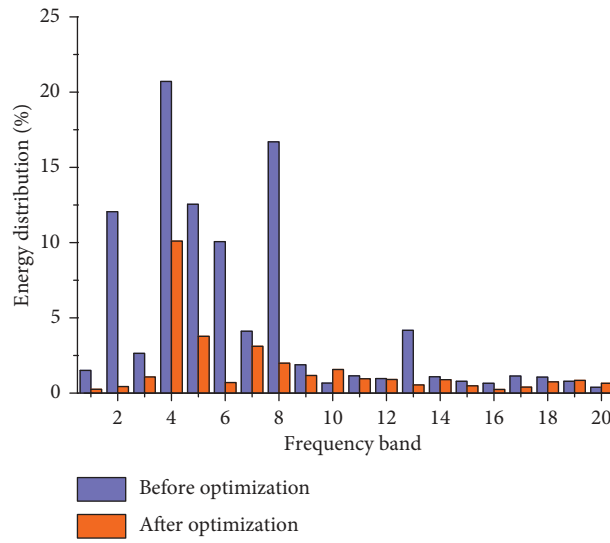

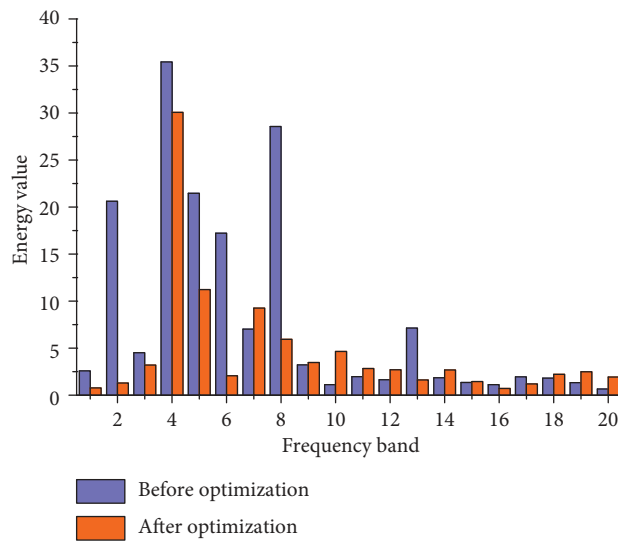FIGURE 22: Energy percentage with frequency band distribution.

FIGURE 23: Energy value with frequency band distribution.

6. Conclusions

Based on the background of the Dizong tunnel of the An-Liu high-speed railway, this paper studies the controlled blasting technology of the super-large section tunnel passing through houses at close range and proposes an optimized blasting scheme. The wavelet (packet) analysis technique is used to compare and analyze the power spectrum characteristics and energy distribution characteristics of the blasting signals of the two schemes before and after optimization. The conclusions are as follows:

(1) The monitoring data of the blasting test area show that the vertical vibration velocity of the blasting is greater than the horizontal vibration velocity, and the vibration velocity of the blasting distance between 65 and 70 m is between 1.2 and 1.4 cm/s, which is greater than the maximum allowable vibration velocity of 1.2 cm/s. The peak velocity of the blasting control area is predicted, and the maximum vibration velocity is 1.63 cm/s. It can be seen that the existing blasting scheme has not met the design standards.

(2) Based on the blasting propagation law of the blasting test area, a blasting optimization scheme combining single-segment maximum charge, multistage duplex wedge groove, adding damping hole, and millisecond blasting is proposed. The field test results show that the optimized blasting scheme produces a maximum vibration velocity of 1.12 cm/s, below the maximum allowable vibration velocity of 1.2 cm/s, and meet the design standards.

(3) Compared with the original scheme, the frequency generated by the optimized scheme is more advantageous. Firstly, the frequency range is increased from 20~110 Hz to 50~150 Hz, which is much higher than the natural vibration frequency of the house and will not cause resonance. Secondly, the maximum vibration intensity produced by the latter is reduced by 79.8% compared with the former, which can effectively reduce the vibration intensity and ensure the safety of existing buildings.

(4) Based on the time-energy analysis, the differential delay of the two blasting schemes is basically the same as the blasting detonator delay time, but the maximum energy value is different, and the latter is 67.75% smaller than the former. Therefore, the millisecond blasting, controlling the maximum single-segment charge and creating the free-facing surface as much as possible, can effectively reduce the blasting vibration, realize the delayed release of the blasting energy, and realize the interference and staggered peak of the blasting vibration.

(5) The vibration velocity of the original scheme has multiple peaks with the frequency band distribution, and the corresponding frequency domain is more dispersed. After optimization, the peak value decreases, and the distribution of the vibration velocity

with the frequency band tends to be gentle. In the energy analysis, the dominant energy of the blasting vibration of the two schemes is distributed in multiple frequency bands. The vibration energy of the former is mainly concentrated in the range of 15.6~124.8 Hz, and the energy of the latter is mainly concentrated in the range of 31.2~218.4 Hz, but in terms of the energy value, the energy value of the latter in the frequency band corresponding to the dominant energy of the former is reduced by 97.81%, 71.49%, 82.44%, 95.93%, and 93.03%, respectively. It shows that the latter can significantly reduce the energy amplitude and reduce the energy concentration phenomenon.

Data Availability

The data used to support the findings of this study are available from the corresponding author upon request.

Conflicts of Interest

The authors declare that there are no conflicts of interest regarding the publication of this paper.

Acknowledgments

References

[1] J. X. Lai, J. L. Qiu, H. B. Fan et al., "Fiber bragg grating sensors-based in-situ monitoring and safety assessment of loess tunnel," *Journal of Sensors*, vol. 2016, Article ID 8658290, 10 pages, 2016.

[2] X. Liu, Y. Han, D. Li et al., "Anti-pull mechanisms and weak interlayer parameter sensitivity analysis of tunnel-type anchorages in soft rock with underlying weak interlayers," *Engineering Geology*, vol. 253, pp. 123–136, 2019.

[3] Y. Cheng, Z. P. Song, J. F. Jin, and T. T. Yang, "Attenuation characteristics of stress wave peak in sandstone subjected to different axial stresses," *Advances in Materials Science and Engineering*, vol. 2019, Article ID 6320601, 11 pages, 2019.

[4] J. B. Wang, W. W. Li, and Z. P. Song, "Development and implementation of new triangular finite element based on MGE theory for bi-material analysis," *Results in Physics*, vol. 13, p. 102231, 2019.

[5] R. Nateghi, "Evaluation of blast induced ground vibration for minimizing negative effects on surrounding structures," *Soil Dynamics and Earthquake Engineering*, vol. 43, no. 12, pp. 133–138, 2012.

[6] T. Wang, Z. P. Song, J. Y. Yang, J. B. Wang, and X. G. Zhang, "Experimental research on dynamic response of red sandstone soil under impact loads," *Geomechanics and Engineering*, vol. 17, no. 4, pp. 393–403, 2019.

[7] M. E. Oncu, B. Yon, O. Taskiran, and T. Taşkıran, "Investigation of blast-induced ground vibration effects on rural

buildings," *Structural Engineering and Mechanics*, vol. 54, no. 3, pp. 545–560, 2015.

[8] Y. W. Zhang, X. L. Weng, Z. P. Song, and Y. F. Sun, "Modeling of loess soaking induced impacts on metro tunnel using water soaking system in centrifuge," *Geofluids*, vol. 2019, Article ID 5487952, 17 pages, 2019.

[9] H. S. Jung, K. S. Jung, H. N. Mun, B. S. Chun, and D. H. Park, "A study on the vibration propagation characteristics of controlled blasting methods and explosives in tunnelling," *Journal of the Korean Geoenvironmental Society*, vol. 12, no. 2, pp. 5–14, 2011.

[10] Z. P. Song, S. H. Li, J. B. Wang et al., "Determination and application analysis of equivalent load of blasting vibration considering millisecond delay effect," *Geomechanics and Engineering*, vol. 15, no. 2, pp. 745–754, 2018.

[11] A. Henningsson, "A model for vibration monitoring of immovable art in churches: reflections on monitoring as a tool for preventive conservation," *Studies in Conservation*, vol. 63, no. 1, pp. 113–120, 2018.

[12] R. Nateghi, "Prediction of ground vibration level induced by blasting at different rock units," *International Journal of Rock Mechanics and Mining Sciences*, vol. 48, no. 6, pp. 899–908, 2011.

[13] J. S. Lee, S. K. Ahn, and M. Sagong, "Attenuation of blast vibration in tunneling using a pre-cut discontinuity," *Tunnelling and Underground Space Technology*, vol. 52, pp. 30–37, 2016.

[14] T. C. Wang, C. Y. Lee, and I. T. Wang, "Analysis of blast-induced ground vibration under surface explosion," *Journal of Vibroengineering*, vol. 16, no. 5, pp. 2508–2518, 2014.

[15] S.-H. Chen, S.-W. Hu, Z.-H. Zhang, and J. Wu, "Propagation characteristics of vibration waves induced in surrounding rock by tunneling blasting," *Journal of Mountain Science*, vol. 14, no. 12, pp. 2620–2630, 2017.

[16] V. Ozacar, "New methodology to prevent blasting damages for shallow tunnel," *Geomechanics and Engineering*, vol. 15, no. 6, pp. 1227–1236, 2018.

[17] J.-G. Kim and J.-J. Song, "Abrasive water jet cutting methods for reducing blast-induced ground vibration in tunnel excavation," *International Journal of Rock Mechanics and Mining Sciences*, vol. 75, pp. 147–158, 2015.

[18] Q. Liang, J. Li, D. Li, and E. Ou, "Effect of blast-induced vibration from new railway tunnel on existing adjacent railway tunnel in Xinjiang, China," *Rock Mechanics and Rock Engineering*, vol. 46, no. 1, pp. 19–39, 2013.

[19] X. H. Li, Y. Long, C. Ji, M. S. Zhong, and H. B. Zhao, "Study on the vibration effect on operation subway induced by blasting of an adjacent cross tunnel and the reducing vibration techniques," *Journal of Vibration Engineering*, vol. 15, no. 3, pp. 1454–1462, 2013.

[20] Z. Q. Li and Z. Li, "Study on the blasting excavation method of urban shallow tunnel," *Applied Mechanics and Materials*, vol. 580–583, pp. 1051–1055, 2014.

[21] L. X. Xie, W. B. Lu, J. C. Gu, and G. H. Wang, "Excavation method of reducing blasting vibration in complicated geological conditions," *Shock and Vibration*, vol. 2018, Article ID 2518209, 12 pages, 2018.

[22] A. Li, Q. Fang, D. L. Zhang, J. W. Luo, and X. F. Hong, "Blast vibration of a large-span high-speed railway tunnel based on microseismic monitoring," *Smart Structures and Systems*, vol. 21, no. 5, pp. 561–569, 2018.

[23] J. B. Wang, Z. Z. Ren, Z. P. Song, R. K. Huo, and T. T. Yang, "Study of the effect of micro-pore characteristics and saturation degree on the longitudinal wave velocity of sandstone," *Arabian Journal of Geosciences*, vol. 12, no. 13, p. 394, 2019.

[24] G. G. U. Aldas and B. Ecevitoglu, "Waveform analysis in mitigation of blast-induced vibrations," *Journal of Applied Geophysics*, vol. 66, no. 1-2, pp. 25–30, 2008.

[25] H. Ma, H. Wang, C. He, Z. Zhang, and X. Ma, "Influences of blasting sequence on the vibration velocity of surface particles: a case study of Qingdao metro, China," *Geotechnical and Geological Engineering*, vol. 35, no. 1, pp. 485–492, 2017.

[26] J. X. Lai, K. Y. Wang, J. L. Qiu et al., "Vibration response characteristics of the cross tunnel structure," *Shock and Vibration*, vol. 2016, Article ID 9524206, 16 pages, 2016.

[27] L. M. Duan, W. S. Lin, J. X. Lai, P. Zhang, and Y. B. Luo, "Vibration characteristic of high-voltage tower influenced by adjacent tunnel blasting construction," *Shock and Vibration*, vol. 2019, Article ID 8520564, 16 pages, 2019.

[28] R. Nateghi, M. Kiany, and O. Gholipouri, "Control negative effects of blasting waves on concrete of the structures by analyzing of parameters of ground vibration," *Tunnelling and Underground Space Technology*, vol. 24, no. 6, pp. 608–616, 2009.

[29] H. W. Ma, L. M. Wang, L. Z. Chen, and Q. S. Li, "Numerical simulation of earthquake damage in rural masonry buildings," *China Earthquake Engineer Journal*, vol. 35, no. 2, pp. 232–239, 2013.

[30] J.-H. Shin, H.-G. Moon, and S.-E. Chae, "Effect of blast-induced vibration on existing tunnels in soft rocks," *Tunnelling and Underground Space Technology*, vol. 26, no. 1, pp. 51–61, 2011.

[31] J. C. Li, H. B. Li, G. W. Ma, and Y. X. Zhou, "Assessment of underground tunnel stability to adjacent tunnel explosion," *Tunnelling and Underground Space Technology*, vol. 35, no. 35, pp. 227–234, 2013.

[32] X. S. Wang and H. Y. Liu, "Reasonable selection of K in blasting vibration velocity regression analysis and its application," *Journal of Wuhan University of Technology*, vol. 27, no. 11, pp. 103–105, 2005.

[33] GB 6722-2014, *Safety Regulations for Blasting*, Standards Press of China, Beijing, China, 2014.

[34] R. K. Huo, S. G. Li, Z. P. Song et al., "Analysis of vibration response law of multistory building under tunnel blasting loads," *Advances in Civil Engineering*, vol. 2019, Article ID 4203137, 16 pages, 2019.

[35] Y. Z. Yang, Z. S. Shao, J. F. Mi, and X. F. Xiong, "Effect of adjacent hole on the blast-induced stress concentration in rock blasting," *Advances in Civil Engineering*, vol. 2018, Article ID 5172878, 13 pages, 2018.

[36] K. Erarsla, Ö. Uysal, E. Arpaz, and M. A. Cebi, "Barrier holes and trench application to reduce blast induced vibration in seyitomer coal mine," *Environmental Geology*, vol. 54, no. 6, pp. 1325–1331, 2008.